LASER-RIPPLON SCATTERING FROM LECITHIN MONOLAYERS AT THE AIR-WATER INTERFACE

H. BIRECKI and N. M. AMER

Applied Laser Spectroscopy Group, Lawrence Berkeley Laboratory,
University of California, Berkeley, California 94720, USA

Résumé. — Nous avons mesuré la fréquence et le coefficient d'atténuation de ripplons (ondes de surfaces excitées thermiquement) sur les monocouches de L-α-dipalmitoyl phosphatidyl choline à l'interface air-eau. L'existence des phases dans les monocouches en fonction de la température et de la densité superficielle, ainsi que le mécanisme d'atténuation des ripplons sont discutés.

Abstract. — We have measured the frequency and damping coefficient of the spontaneous, thermally excited ripplons on monolayers of L-α-dipalmitoyl phosphatidyl choline at the air-water interface. The dependence of the monolayer phases on temperature and surface coverage is presented and the ripplon damping mechanisms are discussed.

1. **Introduction.** —The study of lipid monolayer systems is of interest for a variety of reasons. Their quasi-two-dimensional nature is of relevance to those interested in phase transition and cooperative phenomena. Furthermore, the understanding of such a basic system is a first step towards the elucidation of the physics of the biologically relevant bilayer lipid membranes.

The conventional techniques for investigating insoluble monolayers include the Langmuir-Adam and the Wilhelmy balance methods [1] where static surface pressure is measured as a function of the surface area per molecule. Dynamic properties such as dilatation viscosity (dynamic surface tension) and surface viscosity are typically deduced from flow through slit studies, damping of oscillations of concentric cylinders, and damping of macroscopic surface waves [1, 2]. The results of these experiments are difficult to interpret because of the rather gross perturbations used to probe the experimental system.

Our experimental approach was to probe the spontaneous, thermally excited surface waves, the so called ripplons, by light scattering [3]. The strength of this technique is that both static and dynamic properties of the monolayer can be elucidated in a reliable fashion and with minimum perturbation.

In the present work we are mostly concerned with the mechanisms of ripplon damping, and with the dependence of the monolayer phase transitions on temperature and surface coverage.

2. **Experimental method.** — Our experimental arrangement is shown in figure 1. A beam, 2 mm in diameter, from an Ar⁺ laser (4 880 Å) or a He-Ne laser (6 328 Å)
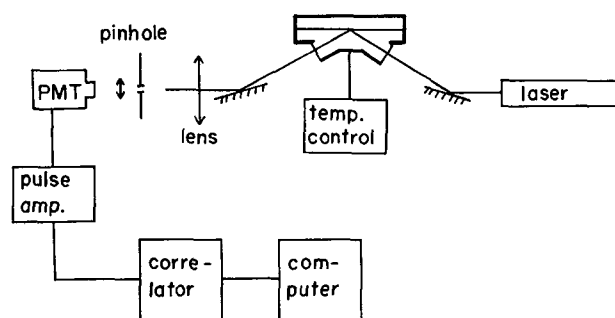

FIG. 1. — Experimental set-up.

probed the air-water interface from the water side. To maximize the signal, the angle of incidence was slightly greater than the angle for total internal reflection [4]. Reflected light was then collected with a 30 cm focal length lens and the scattering wave vector was selected by a pinhole in the focal plane of the lens moving perpendicularly to the plane of the drawing. Light passing through the pinhole was collected on the photocathode of an FW 130 photomultiplier tube and the resulting photocurrent, after pulse shaping and amplification, was analyzed with a 4-bit real time digital correlator. Stray light scattered elastically by windows and other optical components served as the local oscillator. Instrumental linewidth was determined from measurements on pure water and by comparing the results with existing theories [5, 6].

Since ripplons on surfaces form dynamic gratings which phase modulate the reflected beam [7, 8], the scattered light will then be frequency shifted by an amount equal to the ripplon frequency. Due to the

29

small amplitude of the ripplons (few angstroms), light is scattered effectively in the grating's first order, thus allowing for the investigation of one q-vector at a time.

L-α-dipalmitoyl phosphatidyl choline (DPPC) was obtained from Sigma Chemical Co. ($\geqslant$ 98 % purity) and was used without further purification. The mono-layers were deposited on the interface by spreading from a 9 : 1 hexane : ethanol solution (reagent grade). Demineralized distilled water was used for the experiments. The pH was 5.2 $\pm$ 0.2 and the sample temperature was stable to better than 0.1 °C. The air over the interface was routinely purged with nitrogen to minimize DPPC oxidation.

3. **Theory.** — We have extended the hydrodynamic theory of ripplons [5, 6, 9] to insoluble surfactants at interfaces. We take into account the following mono-layer parameters : the static surface tension $\pi(c)$ as a function of surface coverage c ; the dilatational viscosity $\beta(c)$ which takes into account the change in surface tension due to the rate of surface area change [1] ; the intrinsic surface viscosity $\eta_s(c)$; and the slip friction coefficient $\mu(c)$ which accounts for the difference in the velocity of the lipid film and the water [10]. We assume the interface to be in the x-y plane and no motion in the y direction.

The following set of equations then describe an insoluble monolayer :

1. $\nabla.\mathbf{v} = 0$ (water incompressibility).

2. $\rho\, \partial_t \mathbf{v} = - \nabla p + \eta\, \Delta \mathbf{v}$ (Navier-Stokes equation of motion for water).

3. $c\, \partial_t v_L = \dfrac{\partial \pi}{\partial c}\, \partial_x c + (\beta + 2\, \eta_s)\, \partial_x^2 v_L - \mu(v_L - v_x(z = 0))$ (equation of motion of the monolayer).

4. $\partial_t c + c\, \partial_x v_L = D\, \partial_x^2 c$ (continuity equation for surface layer).

5. $v_z(t, x, z = 0) = \partial_t \xi(t, x)$ (velocity boundary condition).

6. $p(z = 0) - 2\, \eta\, \partial_z v_z\, (z = 0) + \pi\, \partial_x^2\, \xi + \beta\, \partial_x^2\, \partial_t \xi = 0$ (boundary condition on normal force acting on interface).

7. $- \eta(\partial_x v_z + \partial_z v_x)\, (z = 0) + \mu(v_L - v_x(z = 0)) = 0$ (boundary condition on tangential force acting on interface).

where

  ξ ripple amplitude
  $\mathbf{v}$ water velocity
  v_L lipid velocity in the x-y plane
  D molecular surface diffusion coefficient
  p hydrostatic pressure
  η water viscosity
  ρ water density.

We look for a solution of the form

$$\xi(x, t) = \xi(t)\, e^{iqx}$$

Following general lines of reference [6], we can solve the above equation in terms of their time Laplace transforms. The result is

$$\tilde{\xi}(s) = - \frac{\xi(t = 0)}{s} \times$$

$$\times \left[\frac{\left(\sigma + \dfrac{1}{x}\, \dfrac{\mathcal{E}(x)}{x + d}\right) (1 - m(x) + \theta x) + 1}{\mathfrak{D}(x)} - 1 \right]$$

where

$$\mathfrak{D}(x) = [1 + (x + y)^2 - y^2\, m(x) + Bx] \times$$

$$\times \left[1 + \theta \left(\sigma x + \frac{\mathcal{E}(x)}{x + d}\right) \right] + \left(\sigma + \frac{1}{x}\, \frac{\mathcal{E}(x)}{x + d}\right)$$

$$\times [(1 - m(x))\, (1 + Bx) - x^2\, m(x)]$$

$$x = s/\omega_0$$

$$\omega_0 = \sqrt{\pi q^3/\rho}$$

$$y = 2\, \eta q^2/\pi_0\, \rho$$

$$m(x) = \sqrt[+]{1 + 2\frac{x}{y}}$$

$$\mathcal{E}(x) = \frac{\partial \pi}{\partial c}\, \frac{c}{\pi} + 2\, \eta_s\, q^3(x + d)/\pi_0\, \rho$$

$$d = Dq^2/\pi_0$$

$$B = \beta \omega_0/\pi$$

$$\sigma = cq/\rho$$

$$\theta = \rho \omega_0/\mu q\,.$$

The power spectrum of the ripplons, which is the Fourier transform of the experimentally measured correlation function, is then given [6] by

$$P(\omega) = \frac{\langle\, |\, \xi(t = 0)\, |^2\, \rangle}{\pi \omega}\, \mathfrak{Im}$$

$$\left\{ \frac{1}{\mathfrak{D}(x)} \left[1 + \left(\sigma + \frac{1}{x}\, \frac{\mathcal{E}(x)}{x + d}\right) \right. \right.$$

$$\left. \left. \times\, (1 - m(x) + \theta x) \right] \right\}_{s = -i\omega}.$$

Computer calculations showed that in the range of the parameters of interest, the resulting power spectrum is very nearly Lorentzian and thus the experimental correlation data were fitted to the form

$$C(\tau) = C(0)\, e^{-\Gamma t} \cos (\omega t + \varphi)$$

where the additional phase φ was needed to account for most of the deviation from Lorentzian shape.

4. Results and discussion. — Since, to a first approximation [11, 12], one expects that for a free surface $\omega = (\pi q^3/\rho)^{1/2}$ and $\Gamma = 2\,\eta q^2/\rho$; therefore our data (Fig. 2) are plotted as apparent surface tension $\pi = \omega^2\,\rho/q^3$, and relative damping constant $g = \Gamma/2\,vq^2$. For surface coverage larger than 0.01 mol./Å², the surface tension rapidly decreases as the number of molecules per unit area is increased until the transition region between the expanded and condensed phases of the film is reached. This is exhibited by an abrupt change in the slope of the
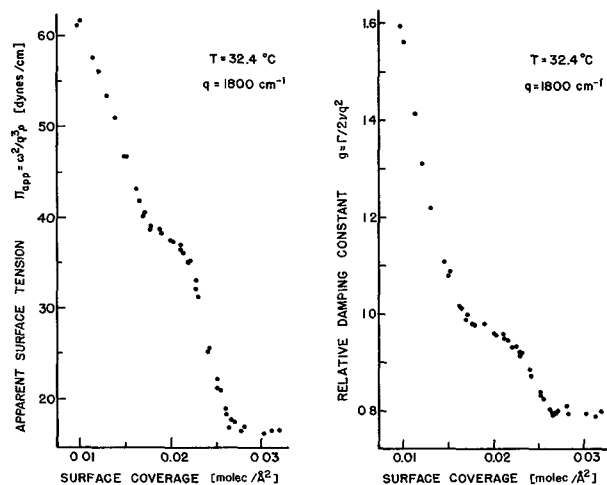

FIG. 2. — Apparent surface tension and damping as a function of surface coverage for 32.4 °C.

apparent surface tension vs coverage curve at the low coverage side, while at the high coverage end of this region the transition to the condensed phase is gradual. Further increase of surface coverage results in a rapid decrease in the surface tension. Once the full monolayer is reached addition of more molecules does not change the value of the observed surface tension.

The behaviour of the damping constant is qualitatively similar to that of the apparent surface tension. It should be noted that at lower temperatures the shoulder corresponding to the expanded-condensed transition becomes much less pronounced.

No measurements are shown for coverages of less than 0.01 mol./Å². Below that, the results were not reproducible and varied over a large range of values within a few minutes. This suggests the presence of two coexisting phases (gaseous and liquid) with average size larger than the laser beam diameter.

The theory described in section 3 is a function of several dissipation parameters the relative importance of which can now be estimated.

We estimate the slip parameter μ to be the ratio of the water viscosity η and the mean distance between the lipid molecules; i.e., $\sim 10^5$ P/cm. For our range of wave vectors, calculations shows that Γ was independent of μ for $\mu > 10^3$ P/cm. Thus slip is unimportant in our case. We can also neglect the dilatational viscosity since in our range of q's the results show no q^3 dependence for Γ, which would be the case if dilatational viscosity were important.

Published values for surface viscosity of the expanded phase fall in the range of 10^{-4} and 10^{-3} surface poise, and for the condensed phase they are on the order of 1 surface poise [13, 14]. From our data, we estimate the surface viscosity for the expanded phase to be $< 10^{-5}$ surface poise, otherwise the theoretical q-dependence of the damping constant will be in large disagreement with the observed values and our high damping values at low coverage could not be accounted for. The damping in the expanded phase is thus due to the particular combination of surface compressibility and surface tension.

In the condensed phase our results are consistent with the behaviour of an incompressible film. However, since the compressibility values derived from our surface tension data are too large to account for an incompressible behaviour, therefore we are lead to conclude that surface viscosity is an important damping mechanism in the case of the condensed phase and that it is $> 10^{-3}$ surface poise. To verify this conclusion, data at smaller q's than we have been able to achieve are needed.

In figure 3 we give the q-dependence of the relative damping coefficient for two coverages at 26 °C. Figure 3a shows the results for a coverage of 0.013 5 mol./Å² with a surface tension of 60.5 dynes/cm. The theoretical curve is for zero surface viscosity and a film compressibility of 0.02. In figure 3b we give the results for a coverage of 0.022 3 mol./Å² with corresponding surface tension of 39 dynes/cm. The theoretical curve in this case is for an incompressible film at the interface. For q values above 10^3 cm^{-1}, the experimental results agree with the theoretical fit for both coverages. The systematic discrepancy between theory and experiment for the lower q's is caused, in part, by an overestimate of the instrumental linewidth due to our inability to completely isolate low frequency mechanical vibrations from our experimental set-up.

In figure 4 we present a summary of the temperature dependence of the real surface tension, the relative damping coefficient, and the area per molecule for both a full monolayer and for the low coverage side of the expanded-condensed transition region. It can be seen that the low coverage results extrapolate to the full monolayer values at $\sim$ 42 °C. It is of interest to note that, for a full monolayer, an 8 Å² jump in the area per molecule occurs within an increment of one degree around 41 °C. This provides evidence that the expanded-condensed phase transition is in fact the chain melting one observed at 41.5 °C in bulk DPPC [15, 16]. The magnitude of the jump is consistent with bulk X-ray data [15].

We observe no increase in the compressibility of the monolayer at the onset of the expanded-condensed
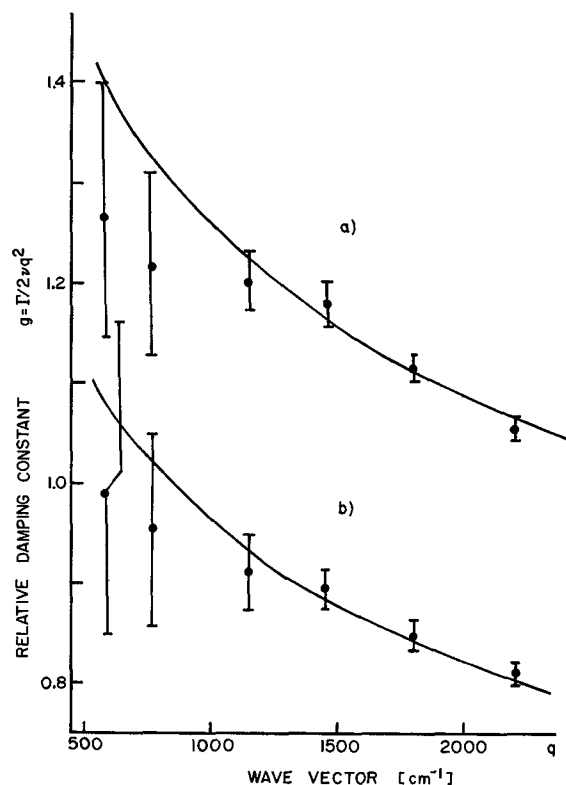
FIG. 3. — Wave vector dependence of relative damping coefficient at 26 °C. a) Coverage of 0.013 5 mol./Å^2 (expanded phase), b) coverage of 0.022 3 mol/Å^2 (condensed phase) ; the solid lines are theoretical fits for zero surface viscosity and for an incompressible film, respectively.

transition as the temperature increases. This, and the jump in area per molecule, lead us to conclude that the system does not exhibit critical behaviour.

It is known that a second phase transition, the so called pretransition, occurs in bulk DPPC systems at 34.5 °C [16-18]. We observed such a transition in the monolayers. Our evidence for that is the abrupt change in the slope of the surface tension vs temperature isochore as shown in figure 5.

FIG. 5. — Surface tension isochore showing the pretransition. Only some of data points are shown. The solid line represents the average behaviour of data.
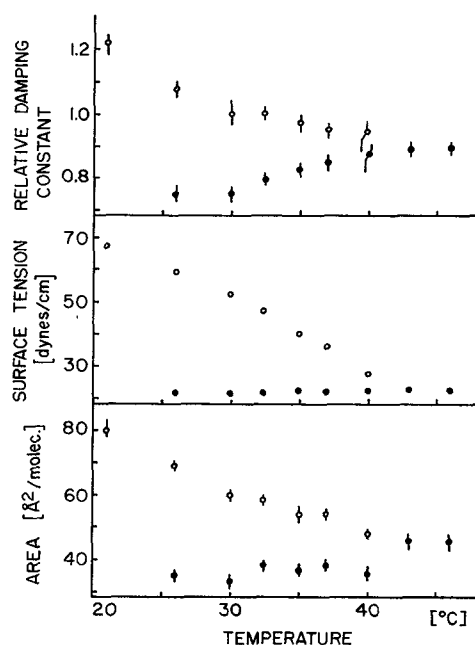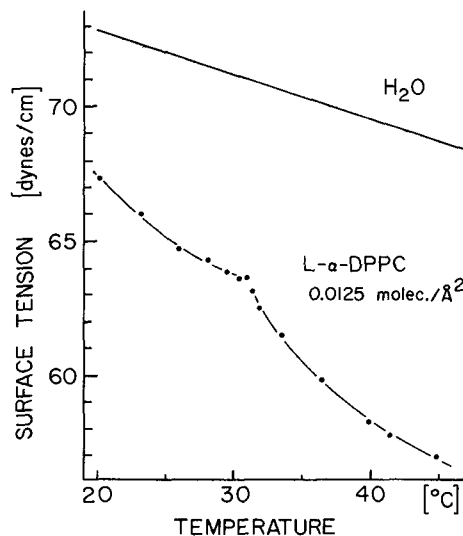

FIG. 4. — Temperature dependence of monolayer parameters. Solid circles are for full monolayer, open circles for the low coverage side of the expanded-condensed transition region.

Albrecht et al. have recently published a phase diagram of DPPC monolayers [19] which exhibits an isotropic-anisotropic fluid transition within the expanded state. We should like to point out that this is not the same transition shown in figure 5. According to reference [19] the isotropic-anisotropic transition takes place at surface pressures above 10 dynes/cm as compared with 7.4 dynes/cm in our case. In addition, the transition line of reference [19] moves towards high surface pressures at high temperatures and one would have to observe a second change of phase back to the isotropic state. No such second transition was seen. The fact that at low coverage the transition occurs at a lower temperature is consistent with weaker cooperative interaction at lower densities. The isotropic-anisotropic fluid transition described in reference [19] appears as a discontinuous decrease in the monolayer compressibility as the surface coverage is increased. Such a change should lead to a discontinuous decrease of the ripplon damping which, within the accuracy of our data, we do not observe.

We observe that the film loses stability in the condensed phase about 34 °C for surface tensions lower than about 30 dynes/cm. The temperature dependence of this instability may possibly be related to the pretransition.

_5. **Conclusion.** — The initial results described above show that scattering of light by ripplons can be a useful tool for probing the rheological and phase transition aspects of insoluble monolayers at the interfaces. Further work is in progress in our laboratory.

References

[1] GAINES, G. L., *Insoluble Monolayers at Liquid-Gas Interfaces* (Interscience, New York) 1966.

[2] LUCASSEN, J. and HANSEN, R. S., *J. Coll. Interf. Sci.* **22** (1966) 32.

[3] BOUCHIAT, M. A. and MEUNIER, J., *Polarisation, Matière et Rayonnement* (P.U.F.) 1969.

[4] HERPIN, J. C. and MEUNIER, J., *J. Physique* **35** (1974) 847.

[5] PROSPERETTI, A., *Phys. Fluids* **19** (1976) 195.

[6] BOUCHIAT, M. A. and MEUNIER, J., *J. Physique* **32** (1971) 561.

[7] HARD, S., HAMNERINS, Y. and NILSSON, O., *J. Appl. Phys.* **47** (1976) 2433.

[8] LEAN, E. G. in *Progress in Optics* (Wolfe, E., edit. North-Holland) 1973.

[9] LANGEVIN, D. and BOUCHIAT, M. A., *C.R. Hebd. Séan. Acad. Sci. B* **272** (1971) 1422.

[10] BROCHARD, F. and DE GENNES, P. G., *Parmana* Suppl. **1** (1975) 1.

[11] LANDAU, L. D. and LIFSHITZ, F. M., *Fluid Mechanics* (Addison-Wesley, Mass.) 1959.

[12] LEVICH, V. G., *Physicochemical Hydrodynamics* (Prentice Hall, N.J.) 1962.

[13] PHILLIPS, M. C., CHAPMAN, D., *Biochem. Biophys. Acta* **163** (1968) 301.

[14] HAYASHI, M., MURAMATOU, T., HARA, I., SEIMIYA, T., *Chem. Phys. Lipids* **15** (1975) 209.

[15] RAND, R. P., CHAPMAN, D., LARSSON, K., *Biophys. J.* **15** (1975) 1117.

[16] JANIAK, M. J., SMALL, D. M., SHIPLEY, G. G., *Biochemistry* **15** (1976) 4575 and references therein.

[17] UHING, M. C., *Chem. Phys. Lipids* **14** (1975) 303.

[18] GALLY, H. U., NIEDERBERGER, W., SEELIG, J., *Biochemistry* **14** (1975) 3647.

[19] ALBRECHT, O., GRULER, H., SACKMANN, E., *J. Physique* **39** (1978) 301.